



FMCW GPR radar for archaeological applications: First analytical and measurement results

Manuel A. Yarlequé, Sthefany Alvarez, Hansel J. Martínez and Aldo C. Canelo
Pontificia Universidad Católica del Perú, Departamento de Ingeniería, Lima, Perú

Abstract

This paper describes a Ground Penetrating Radar (GPR) using frequency modulated continuous wave (FMCW) technique which produces 2D images for archeological detection. This radar operates at 745 MHz, with a bandwidth of 510 MHz. For a first evaluation of the GPR system, a structure was set up to emulate the flight of an Unmanned Aerial Vehicle (UAV).

The radar is capable of acquiring and storing data in order to do a post-processing using range migration algorithm (RMA). The results are evaluated by imaging a metal plate of 50 cm of diameter with a burial depth of 0.3 meters.

1. Introduction

In the field of Archeology one of the most important tasks is to locate and record archaeological sites and buried objects, using a system to acquire underground images. The use of photographic images for this purpose is restricted to the availability of natural light and good atmospheric conditions. The use of a traditional ground penetrating radar (GPR) is not convenient due to the difficult access as well as to the conditions of intangible areas. The aim of this project is to develop an FMCW radar architecture for the detection of images in Archeology. First, the hardware stages of the radar and the processing was implemented, in order to perform GPR configuration the integration and testing of the system was set up. The preliminary results were developed using a test-site structure to evaluate and emulate the performance of a UAV flight. This radar will be mounted in a mini-UAV for GPR testing on campus as well as at archaeological sites.

2. Background

Previously, a FMCW radar was developed and signal processing was performed using SAR techniques in air generating 2D images for fixed targets. This SAR system achieve fine along-track resolution taking several range profiles to synthesize an aperture length [1]. The radar and the size of antennas were designed to be used in mini-UAVs. The data collection geometry describes along-track and crossrange axes to enhances resolution of the image. The data is digitalized and stored "onboard". RMA techniques was used for image formation [1].

3. Mathematical Modeling of deramp processing

The FMCW GPR transmits periodic frequency modulated continuous wave which is scattered off the target and collected by the receiver antenna. This signal sweeps linearly as a ramp waveform from an initial frequency (f_0) during a sweep period of time T [2]:

$$f_s(t) = f_0 + \alpha t \quad t < T \quad (1)$$

Where α is the radar chirp rate, the transmitted signal can be expressed as:

$$T(t) = \cos\left(\omega_0 t + \frac{\alpha}{2} t^2 + \phi(t)\right) \quad (2)$$

The phase distortion is represented by $\phi(t)$ and the received signal is composed of waves from the surface and underground layers. This reflected signal is delayed by τ from the transmitted signal:

$$T(t) = \cos\left[\left(\omega_0 + \frac{\alpha}{2}(t + \tau)\right)(t + \tau) + \phi(t + \tau)\right] \quad (3)$$

The frequency difference generated by multiplying the transmit and receive signals, then is filtered to remove additional frequencies:

$$u_{IF} \approx \cos\left[\omega_0 \tau + \alpha \tau t + \frac{\alpha}{2} \tau^2 + \phi(\tau)\right] \quad (4)$$

The beat frequency is directly related to the time delays τ of the reflected signals by the equation:

$$\delta_f = \alpha \tau = \frac{2RB}{vT} \quad (5)$$

Where v is the propagating velocity, and because of lineal modulation the chirp rate is a ratio of bandwidth over chirp time.

4. System Implementation

The system is composed of a rail structure with a length of 2.5 m, a height of 1.5 m and 1.5 m of width (to emulate the flight of an UAV) with a maximum separation between the antennas and soil target of 1 meter. The system is evaluated in a kind of ground of homogenous clayey dry soil where a metal plate was buried in order to perform test measurement. This material is located on top of the natural bedrock (Figure 1). The clayey soil has a dielectric permittivity range from 4 to 6. This produces changes in the velocity of propagation waves as shown in the following formula [2]:

$$v = \frac{c}{\sqrt{\epsilon_r}} \quad (6)$$

Furthermore, these permittivity changes may cause errors of distance measurement according to the type of target to detect.

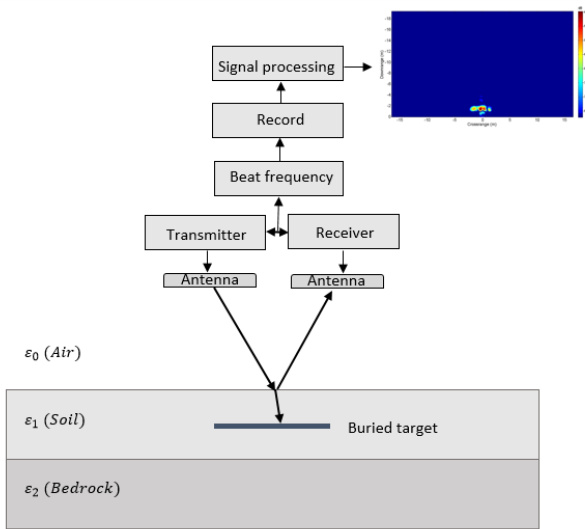


Figure 1. FMCW GPR Test System

4.1 Test site setup

This FMCW radar is compact in dimensions, portable and exhibit low energy consumption, so it can be integrated as a part of mini UAV capable of a payload less than 3 kg.

In Figure 2, the structure used for characterizing the radar is shown. The test field covers a fixed track of 1.5 m length and it is at 1 m from soil to simulate the flight altitude of the UAV.

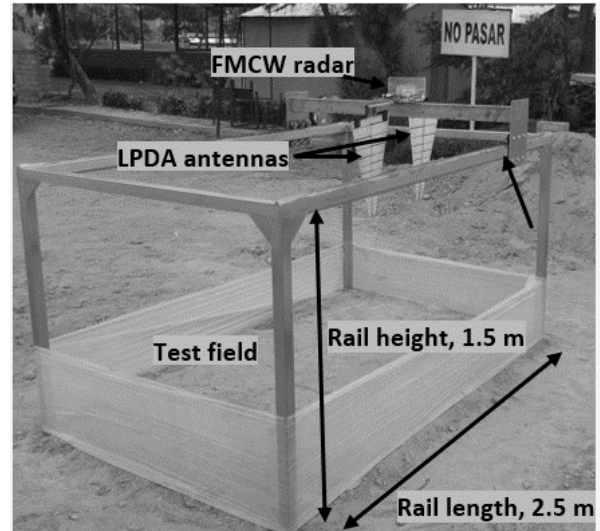


Figure 2. FMCW GPR Test System.

4.2 System Overview

In this FMCW GPR, the transmitter frequency sweeps from 490 MHz to 1000 MHz in a half period of the modulating ramp waveform (30 ms). The length of the time window for spectrum analysis is shorter than a half of the modulation period. The radar allows to select the frequency band used for imaging; the higher frequency, the shorter wavelength, then better resolution.

A delay time T is detected as a peak at frequency of beat frequency ($fb=aT$) in the power (amplitude) spectrum of the beat signal in the FMCW radar; furthermore, the delay time T also appears in the phase term of the spectrum. Therefore, another image using phase spectra can be extracted. In a phase spectrum by FFT, a step-like change of phase appears at a frequency corresponding to the delay time T [4]. Since there are some cases where detection of step-like change is easier and more accurate than peak detection, a FFT phase spectrum image of the FMCW GPR is obtained.

5 Measurement results

In the FMCW GPR, a deeper target appears in higher frequency domain. It is well known that differentiating time-varying signal results in emphasizing the higher frequency part of its power spectrum [5]. By differentiating a beat signal of the FMCW GPR, deeply buried targets appears more clearly in the GPR image.

In Figure 3, an A-scan of a buried target is represented at 0.3 meters. It has several samples per time to improve the resolution of the image. This was filtered to remove clutter that appeared due to the characteristics of the soil, then there were additive beat frequencies that superposed the reflected signal of the target.

Many spectral-estimation methods such as FFT, MEM, etc., [5] are applicable for detecting the beat frequencies.

They have both advantages and limitations, respectively; so, a proper method was chosen for the purpose.

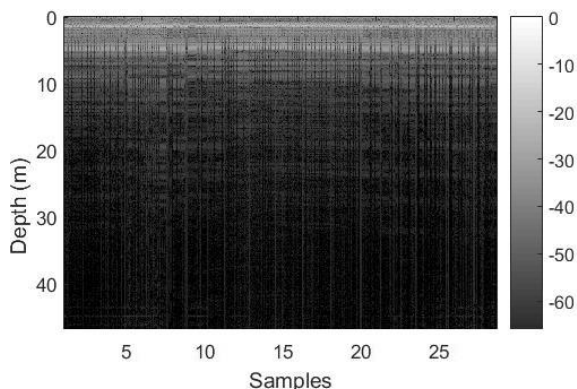


Figure 3. A-Scan image of raw data processed for buried metal object.

After data collection of several range profiles in a test field area, an autofocused 2D B-Scan image is demonstrated (see Figure 4.), it is performed for a synthetic aperture of 1.5m and a set of 30 discrete A-scan. The return from the buried target appears as the hyperbola in the space-time GPR image since path of the EM wave varies as the GPR radar sensor moves along the surface.

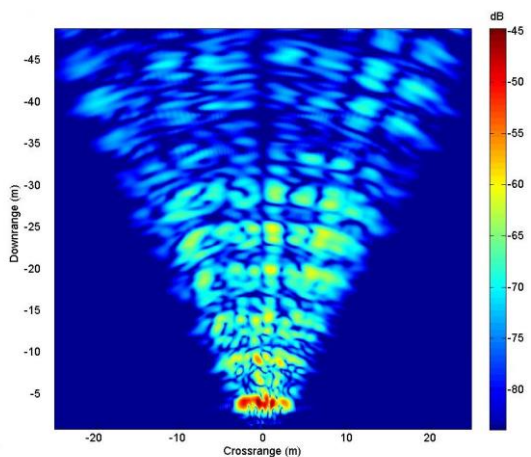


Figure 4. B-scan for buried target.

A preliminary formed image is illustrated in figure 5. for the same buried target in the same clayey-dry soil environment. Since the data are collected over a 2D aperture on top of the surface at 1m of height.

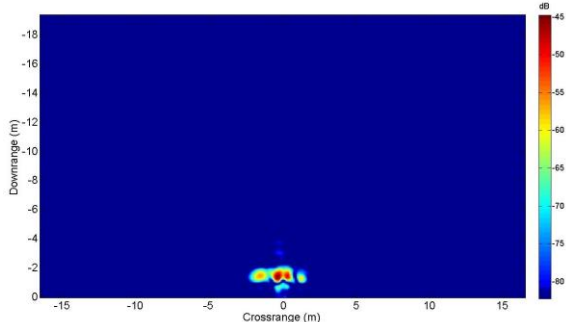


Figure 5. SAR processed image for buried metal object.

6. Conclusion

The operability of a FMCW GPR system using a structure to emulate the UAV path has been demonstrated. This system was designed and implemented to evaluate the performance of a portable radar to acquire and store data for a post-processing imaging. A buried metal plate was used to achieve a correct detection and to enhance the response in image processing. Correspondence between distances obtained by radar (1.3 meters), and distances measured manually (1.2 meters), show the correct performance of radar to locate metal targets.

In a future work we expect test the radar mounted in an UAV, to demonstrate the final functionality of this GPR FMCW radar.

7. Acknowledgements

This work was supported by the Fondos para la Innovación, Ciencia y Tecnología (FINCyT-Peru) under CONTRACT N 121-PNCP-PIAP-2015.

8. References

1. W. G. Carrara, R. S. Goodman, and R. M. Majewski, Spotlight Synthetic Aperture Radar Signal Processing Algorithms, Norwood, MA, Artech House, 1995.
2. G. L. Charvat, A Low-Power Radar Imaging System, PhD dissertation, Department of Electrical and Computer Engineering, Michigan State University, East Lansing, MI, 2007.
3. H. M. Jol, Ed., Ground Penetrating Radar Theory and Applications, 1st ed. Amsterdam, The Netherlands: Elsevier, 2009.
4. G.L. Charvat, Small and Short Range Radar Systems, Series on Practical Approaches to Electrical Engineering, CRC Press, 2014.
5. C. Ozdemir, Inverse Synthetic Aperture Radar Imaging with MATLAB Algorithms, Mersin University, Turkey, Wiley, 2012.